DOI: 10.14621/ce.20170205

Effect of the Cellular Communication Mast Structure on the Wind Speed Measurement Results

Valerijs Bezrukovs[1,2], Sabine Upnere[2], Vladislavs Bezrukovs[2]*, Aleksejs Zacepins[1], Normunds Jekabsons[2]

[1]Institute of Physical Energetics
11 Krivu, Riga LV-1006, Latvia; elmag@inbox.lv

[2]Ventspils University College
101 Inzenieru, Ventspils LV-3601, Latvia; vladislavsb@venta.lv

Abstract

This paper discuss possibility to use existing and widely distributed tall cellular communication masts for wind speed measurements. Cellular communication masts are similar to the metrological mast proposed for wind measurements. Main difference is additional vertical cable lines installed inside the mast what increase solidity of entire mast structure and as a result may introduce unacceptable errors in the wind speed measurements from mounted sensor. Influence of this cable lines to the wind speed measurement results was explored by CFD modelling of air flow around the mast. The CFD modelling results are obtained for simulations of air flow interaction with a triangular lattice mast, taking into account the cable lines and compared with wind flow interaction with generic metrological mast. The different types of cellular communication masts are considered along with estimation of their possible use for wind resource assessment. The motivation of this study is to calculate the distance from the mast centre to the boundary of the area where the distortions of the air flow does not exceed ±1% as it is defined by the IEC standard.
The CFD modelling of the flow field around one section of mast has been done using the OpenFOAM open source software. The 3D model of the mast used in the simulation consists of three cylindrical main beams, smaller connecting beams, a ladder, and cables. The results of the authors' studies are illustrated by colour maps of wind flow distribution around a mast (side width 0.74 *m*) for wind speeds *U* = 5.0 and 10.0 *m/s* and for 12 wind flow directions relative to the position of the boom with sensor. The results are compared with the similar studies and models from IEC standard.

Keywords:	Wind speed measurements; Lattice mast; Turbulent air flow; CFD modelling
Article history:	Received: 07 April 2017 Revised: 25 October 2017 Accepted: 30 October 2017

1. Introduction

Evaluation of the wind energy potential is the starting point for making the necessary decisions before construction of mast is initiated. To save time and expenses for deployment of new wind speed measurement site it is worthwhile to use the existing network of cellular communication masts. This would allow minimizing the installation and assembly costs of the measurement equipment.

At performance evaluation for the designed wind parks (WPPs) mainly measuring complexes are used. They consist of cup sensors and a recording unit, which are positioned on a mast at the site of park construction. To exclude the surface effect, the mast height at investigation of the wind energy potential should be not less than 30 *m* [1]. At the same time, in compliance with the requirements set by the international standard IEC 61400-12-1 – Wind turbines, Part 12-1: Power performance measurements of electricity producing wind turbines – [2]. The standard has been created to provide uniform methodology to ensure consistency, accuracy and reproducibility in the measurement and analysis of power performance by wind turbines.

It is of importance that the mast structure does not introduce distortions into the air flow that cause > 1% error at measuring the wind speed.

In practice, the task of wind shear investigation can be made much more simple and cheap if as the bearing support the cellular communication masts with measuring sensors are used [3]. In this case it is of interest to investigate the influence of the design elements of these masts on the distribution of air flow and to evaluate the possibility of their use for obtaining reliable information on the wind speed [4, 5].

The recommendations for calculation of the sensor distance from the mast depending on its design are

given in the IEC standard [2]. However, the results reported in [6, 7] evidence that the boom length calculated in compliance with recommendations of the standard is overestimated. This causes problems with reliability of the boom mount rigidity at installation of sensor on the mast.

In this work, authors have investigated the wind flow distribution around the communication masts in dependence on their real sizes and design, taking also into account communication cables placed in them. The extent of the influence exerted by the structural elements of cellular communication masts on the turbulent air flow is analysed via Computational Fluid Dynamics (CFD) modelling of wind flow distribution.

2. Types of cellular communication masts and calculation of the length of a bottom for installation of wind sensor

For the purposes of the cellular communication the masts of tower and guyed types are used.

The tower type masts shown in Figure 1 have a wide base that imparts stability to them. However, the height of such masts is usually only 45 – 70 *m*. These structures also have a wide square or triangular base with 3 – 6 *m* wide sides, while narrowing to 1.2 *m* in their upper part.

Stability of the guyed type masts (Figure 2) is provided by stranded wires that are fastened to the mast at several levels. A mast of the type is usually made in the form of equilateral triangle with rigidity elements in the form of lattices on each side. Of wide use are masts with side width 0.74 – 1.4 *m*. Cellular communication masts of the "Wibe" series are typically with side width 1.0 and 1.2 *m* [8]. The height of masts from this series is up to 80 – 100 *m*, which allows their use for wind shear measurements. Based on the measurement results, the wind energy potential can be estimated for heights up to 150 – 200 *m*.

In compliance with recommendations given in the IEC standard [2], the measuring sensors should be placed at a definite distance from the mast. In so doing, in order to keep the level of wind speed deficit below 100±1% of the air flow value, the wind speed sensor should be offset from the mast centre to a distance determined by the relationship:

$$\mathrm{R} = \frac{\mathrm{L}}{\frac{1-U_d}{(0.062C_T^2+0.076\,C_T)}+0.082} \quad (1)$$

where:

U_d – relative value of wind speed deficit (0.99);

R – Distance of wind speed sensor from the centre of the mast to the point of observation (*m*);

L – Side width of the mast (*m*);

C_T – The assumed trust coefficient.

The IEC standard determines the distortion field based on the trust coefficient, C_T, given by the equation:

$$C_T = 2.1\,(1-t)t \quad (2)$$

where *t* is the mast solidity defined as the ratio of the projected area of all structural members on the side of mast to the total exposed area. Therefore, taking the simulated geometry of a section of the mast it is possible to calculate its solidity. This parameter is affected by the cable lines of communication antennas inside the mast. The horizontal cross-section of a triangular mast of cellular communication with side width *L* and diameters of the load-carrying tubes *A*, *B*, *C* equal to *D* is shown in Figure 3.

Figure 1. Mast of the tower type

Figure 2. Mast of the guyed type

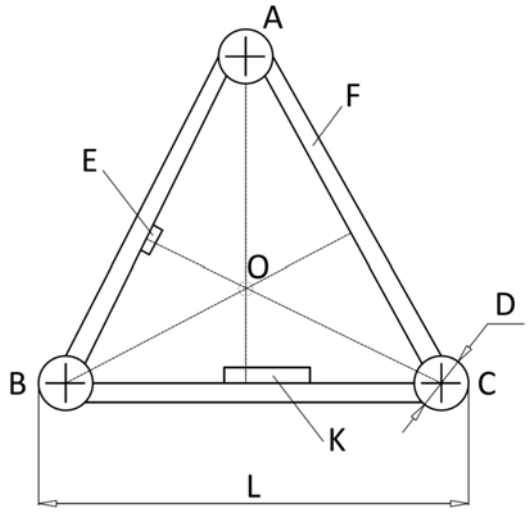

Figure 3. Horizontal cross-section of triangular lattice communication mast: *K* – cable lines; *E* – ladder structure; *O* – mast centre; *F* – mast frame; *D* – diameter of load-carrying tubes

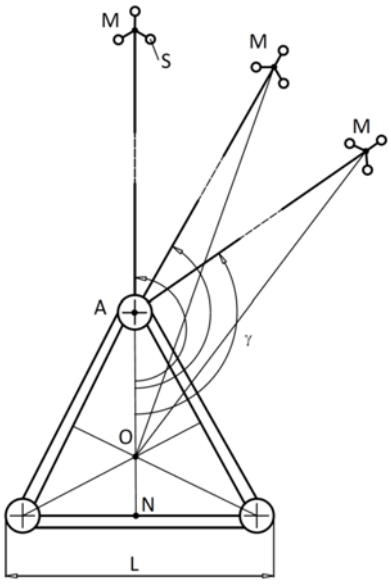

Figure 4. Variants of boom arrangement on the base of lattice communication mast

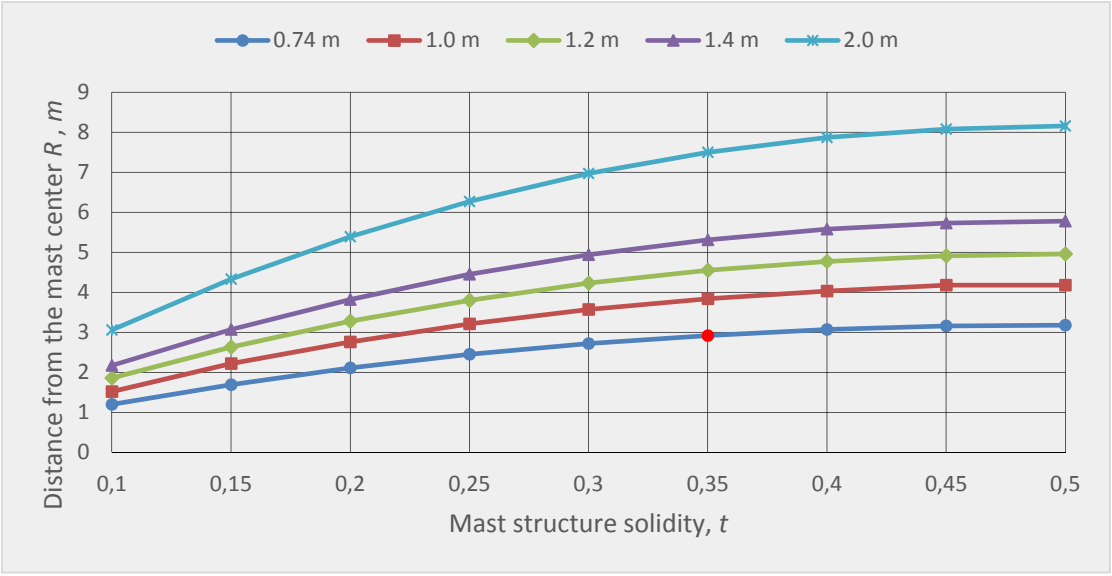

Figure 5. Curves of the distance *R* from the mast centre, *vs.* mast structure solidity *t*

The distance of the sensor from the mast centre depends on the boom position on the supporting structures of the mast. Using known relationships for triangle sides, the vectors in Figure 4 can be expressed as

$$\overline{OM} = R = \sqrt{\overline{OA^2} + \overline{AM^2} - 2\,\overline{OA}\,\overline{AM}\cos\gamma} \qquad (3)$$

$$\overline{OA} = \frac{1}{\sqrt{3}}L, \qquad (4)$$

$$\overline{AN} = \frac{\sqrt{3}}{2}L. \qquad (5)$$

Relationships (3) – (5) for the vectors in Figure 4 make it possible to calculate the distance of sensor *S* from the mast centre *R* in dependence on angle γ. The calculations show that at the boom disposition at angles γ = 120°, 150° and 180° the maximum distance of sensor *S* from the centre can be obtained for angle γ = 180°, while for angles γ = 120° and 150° this distance is smaller by 9% and 2%, respectively.

Using Eqs. (1) and (2) it is possible to calculate the distance from the mast centre to the boundary of the area where the distortion of the air flow value does not exceed ±1%. Figure 5 shows the *R* value depending on the mast structure solidity *t*. The curves are calculated

according to the IEC standard recommendations for masts with side width L = 0.74, 1.0; 1.2; 1.4 and 2.0 *m*.

For the masts of "Wibe" series [8] with the size width 1.0 and 1.2 *m* the solidity of the mast structure without considering cable lines is t = (0.17 – 0.22). These values are in agreement with the calculations given in work [7]. Taking into account the cable lines and the ladder design, this solidity can be t = (0.3 – 0.4). Such being the case, for a mast with the side width L = 0.74 *m* and solidity t = 0.35 we will have R = 3.0 *m*. With account taken for relationships (3) and (4), distance AM in Figure 4 which corresponds to the length of a boom with sensor *S* on top is 2.8 *m*.

However, the results obtained in work [7] evidence that the calculations of distance R using the ICE methodology [2] give only an approximate value. So, for a mast with the side width L = 2.0 *m* and solidity t = 0.17 the corresponding curve in Figure 5 gives the R value of 4.7 *m.*

At the same time, analysis of the results reported in [7] that were obtained using CFD simulations shows that the boundary of the domain where the distortion of air flow speed does not exceed ±1% is at a distance of 3.5 *m*, spreading in 320° limits around the mast, while in the 40° sector the boundary of this domain is at a distance of up to 9.0 *m*.

Similar calculations for the mast of tower type allow for conclusion that, in compliance with the ICE standard recommendations, the wind sensor should be mounted on up to 8.0 *m* boom. In practice, this poses many problems as to the reliability of fixing and inflexibility of such a structure on the mast. Obviously, masts of the tower type are of limited use as the bases for location of measuring sensors.

Consequently, as the object of our investigation the cellular communication masts of guyed type are chosen. For estimation of the influence exerted by these structures on the results of wind speed measurements we will consider the pictures showing CFD simulated distribution of air flow around the masts obtained by modelling.

3. Modelling of wind flow interaction with mast structure

The techniques of CFD are widely applied to predict air flow around structures. For this purpose such methods are used as (Unsteady) Reynolds Averaged Navier-Stokes ((U)RANS), Large Eddy Simulation (LES), etc., to evaluate numerically the interaction between the turbulent fluid flow and the structures.

A computational study of the air flow around a 3D triangular lattice telecommunication mast has been realized using the open source CFD toolkit OpenFOAM. In this study, the construction of mast is modelled as a rigid object. The flow is assumed to be turbulent, incompressible, and isothermal.

The mast consists of three vertical tubular tubes with diameter 0.06 *m* and connecting cross-arms with diameter 0.03 *m* (see Figure 6). Ladders and cables are represented as ellipses. The distance between two vertical tubes, L = 0.74 *m*. The total height of the mast is 92 *m*, with only the top part of the mast being modelled. The boom-mounted anemometers are located at a horizontal distance from the centre of the communication mast.

In Figure 7 (α being the angle of attack) total 12 wind directions with respect to the mast are analysed. For wind flow modelling the directions from the 0°, 90°, 180° and 270° sides are take, with the mast and boom located at angles 0° and ±30° relative to these flows.

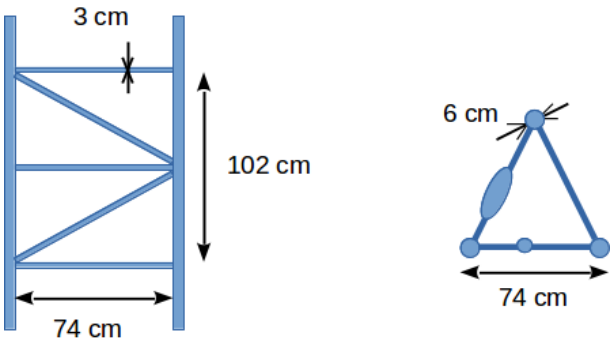

Figure 6. Sketch of analysed triangular lattice communication mast of guyed type and its horizontal cross-section

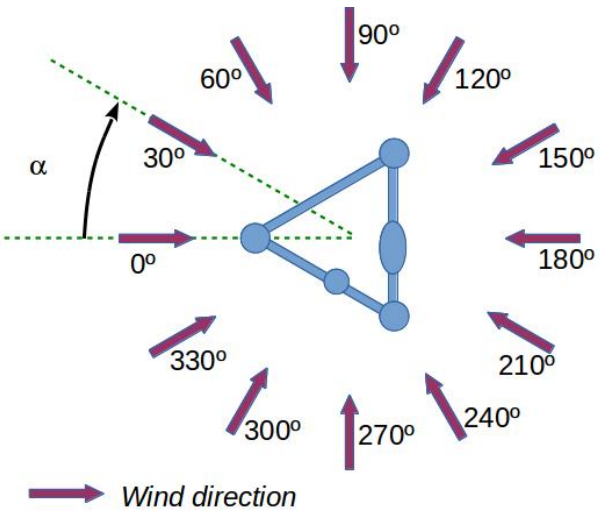

Figure 7. Directions of the wind flows with respect to the triangular lattice mast

For calculations the high-performance computer (HPC) cluster of Ventspils University College was used. The cluster contains total 28 items with two x86 architecture processors with 8 cores for each. The minimum RAM is 32 GB 3-10600R DDR3 and 300 GB 6 Gbps 10000 rpm SAS HDD for the item. In average, one case needs two weeks of computation to achieve the required accuracy.

3.1. Description of the numerical method for flow field prediction

The fluid flow is governed by Navier-Stokes equations and conservation of mass. The effects of the turbulence in the flow are represented by models of turbulence. The finite volume method is used to calculate partial differential equations. The flow field is described by the conservation of mass (Eq. 6) and conservation of momentum (Eq. 7) equations. A time-average approximation has been applied using RANS equations:

$$\frac{\partial \bar{u}_i}{\partial x_j} = 0 \tag{6}$$

$$\frac{\partial \bar{u}_i \bar{u}_j}{\partial x_j} = -\frac{\partial \bar{P}}{\partial x_i} + \frac{\partial}{\partial x_j}\left\{\mu_i\left(\frac{\partial \bar{u}_i}{\partial x_j} + \frac{\partial \bar{u}_j}{\partial x_i}\right) - \rho\overline{u_i' u_j'}\right\} \tag{7}$$

where $\bar{u}$ is the Reynolds-averaged velocity, $\bar{P}$ is the averaged pressure, μ is the eddy viscosity, $u_i' u_j'^{-}$ is the Reynolds stress tensor. This introduces more variables than the number of equations. In order to deal with the system closure problem, two turbulence models are applied: the one-equation Spalart–Allmaras turbulence model and the two-equation standard *k–ε* turbulence model [9]. To couple the pressure and the velocity fields, the SIMPLE technique has been selected using OpenFOAM solver simpleFoam. Standard OpenFOAM wall functions were applied for turbulent viscosity, ν_t, turbulent kinetic energy, *k*, and turbulent dissipation, *ε*.

3.2. Computational domain, mesh and boundary conditions

The three-dimensional computational domain is defined as a rectangular area and has the following dimensions: 30.0 *m* in the streamwise direction, 9.0 *m* in the spanwise direction, and 5.0 *m* in the vertical direction. The computational mesh was generated using the built-in OpenFOAM mesh utilities: *blockMesh* and *snappyHexMesh*. Around the mast surfaces an unstructured mesh is generated, while for the remaining domain part the structured mesh is applied (see Figure 8). In average, the computational domain contains approximately $11 \cdot 10^6$ cells.

As a boundary condition of inflow the constant inlet wind speed, U_∞, is used. The outflow is defined by constant pressure, p = 0. The velocity on the surface walls is equal to zero. At the domain bottom and top the mirror symmetry conditions are applied. The inlet turbulent kinetic energy, *k*, and turbulent dissipation, *ε*, have constant values. The turbulence intensity is assumed to be 15%. For the mentioned parameters (ν_t, *k*, *ε*) standard OpenFOAM wall functions have been applied. The wall function parameter *y+* in average is less than 400 for U_∞ = 10.0 *m/s*, and approximately 200 for U_∞ =5.0 *m/s*.

4. The results of CFD modelling for the interaction of air flow with triangular lattice mast

Due to numerical complexity, a number of simplifications were used for preliminary calculations – such as the first-order accurate numerical schemes; solution are assumed to be converged when the residuals are less than 10^{-5}.

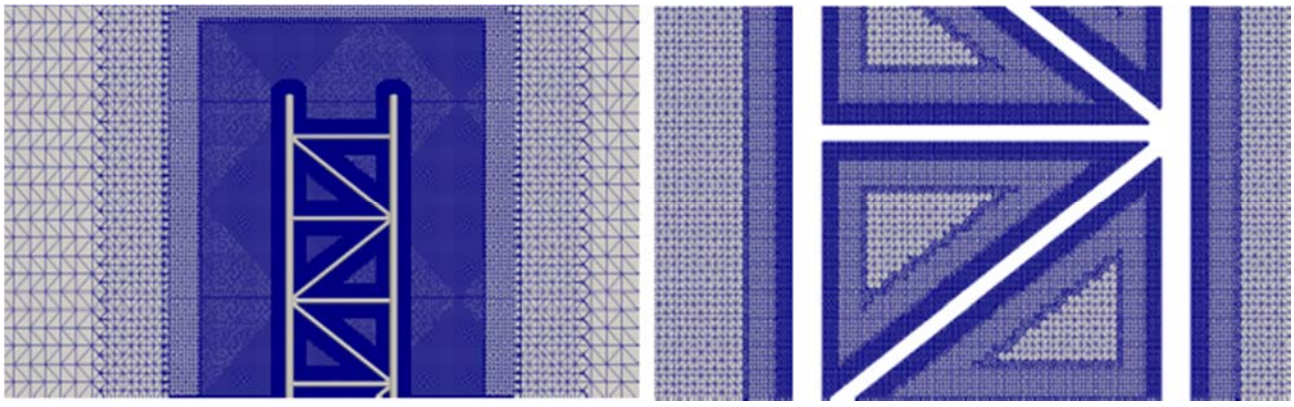

Figure 8. Mesh around the mast surface, vertical cross-section

The results of calculations carried out using HPC are presented as pictures of distribution of coloured fields on which the regions are distinguished where the wind speed deficit does not exceed 100±1.5% at the interaction with a mast with 0.74 *m* wide side.

Figure 9 shows a picture of air flow speed variation at *U* = 10.0 *m/s* and the angle α = 0° relative to the triangular lattice mast. In turn, Figures 10 and 11 demonstrate the speed variations at the air flow interaction with a triangular lattice cellular communication mast with 0.74 *m* wide side at *U* = 5.0 and 10.0 *m/s*. The grey regions in Figures 9 – 11 correspond to the speed of 100±1%, the green-red boundary – to 101.5%, and violet-brown boundary –to 98.5%. Here the flow speed values in the grey, green, and violet meet the IEC standard requirements, while in the red and brown regions the deviations exceed the allowed values.

Position of the sensor *S* is fixed on the mast by a 3.0 *m* boom relative to the triangular mast centre to which the centres of one-metre-step concentric octagons are attached. The boom length corresponds to the red point in Figure 5 for a mast with the side width *L* = 0.74 *m* and solidity *t* = 0.35.

Figures 10 and 11 shows the pictures of air flow distribution for 12 positions of sensor *S* and boom relative to the wind direction at its speeds *U* = 5.0 and 10.0 *m/s*.

In the CFD models it is seen that the presence of cable lines in the triangular lattice cellular communication mast slows down the flow speed more than 1.5% with appearance of a narrow train with angular dimensions are less than 10° with the length of 7.0 – 9.0 *m* (i.e. 10 - 12 widths *L* of mast side). In the limits of 350° sector the region of deviations greater than ±1.5 % does not exceed a distance of 1.5 – 2.0 *m* from the mast centre or 2 – 3 widths *L* of mast side.

As seen from the CFD modelling results, to perform measurements on a mast with the side width *L* = 0.74 *m* and solidity *t* = 0.35 that would comply with the IEC standard it suffices to use a 2.6 *m* long boom. In this case, in the limits of 350° sector the wind speed will be measured with error not greater than ±1.5 %. In turn, in the sector <10° for measurements with the same accuracy the sensor should be at a distance of 9.0 *m* from the mast centre, which is associated with great efforts. While the amount of data obtained in this sector is only 2.5% of the total measurements.

The performed calculations make it possible to refine the results of studies by other authors indicating that the requirements of the IEC standard for the length of the boom are overestimated. At the same time, the simulation results allow us to conclude that the standard do not guarantee the measurement accuracy of ± 1% in the region of train.

5. Conclusions

The CFD modelling of the air flow interaction with triangular lattice cellular communication mast has been executed in compliance with the requirements of the IEC standard. It is shown that for mounting of wind speed measuring sensors the lattice cellular communication masts of guyed type with side width 0.74 *m* can be used.

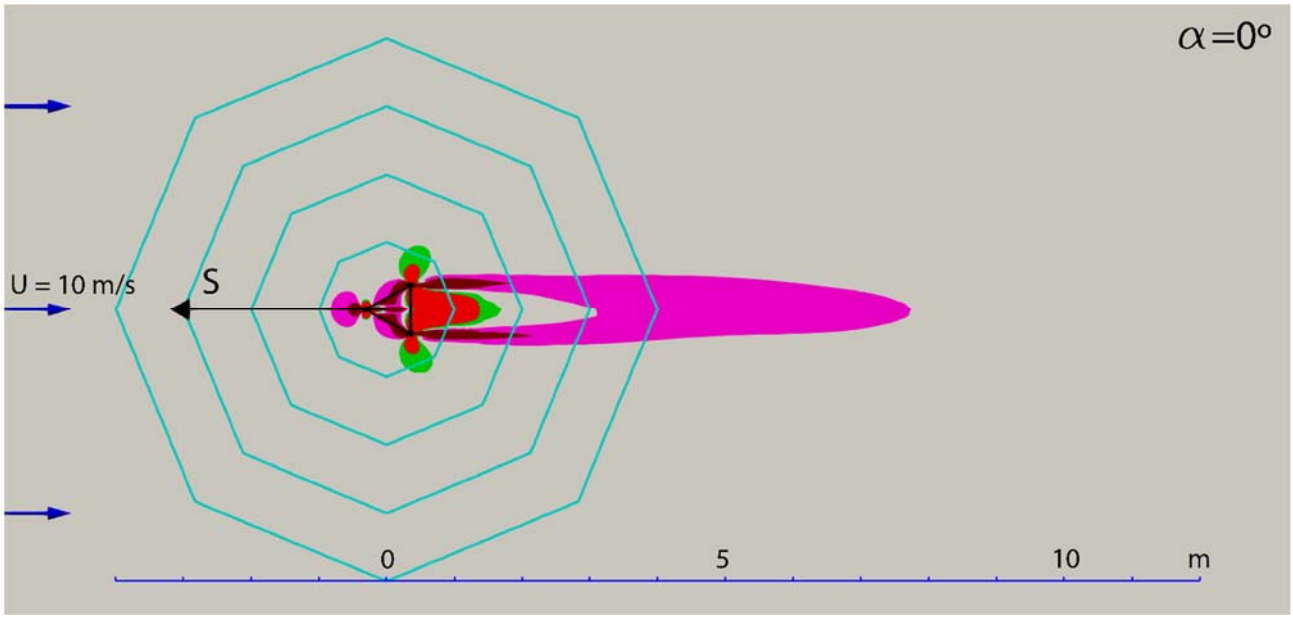

Figure 9. CFD model of the air flow interaction with a triangular lattice mast, side width 0.74 *m*, at the wind speed *U* = 10.0 *m/s* and angle α = 0°, relative to the position of a boom with sensor *S*

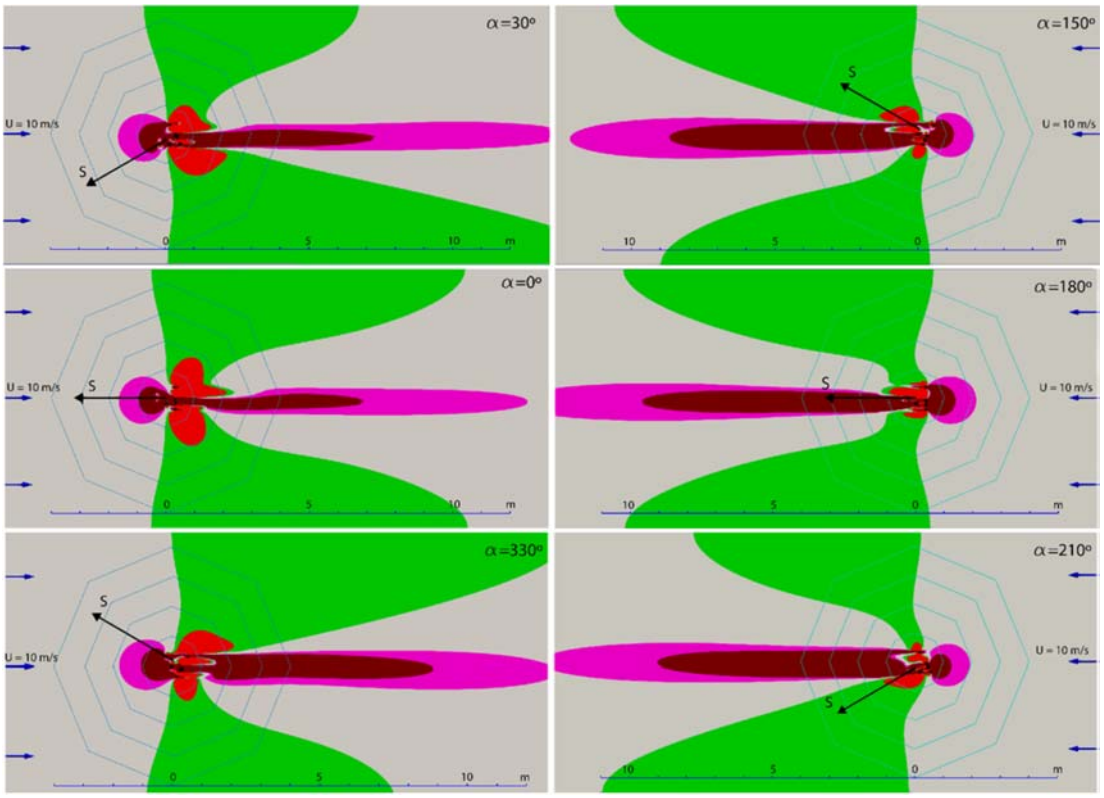

Figure 10 (a). CFD modelling results of the air flow interaction with a triangular lattice mast, side width 0.74 *m*, at the wind speed *U* = 10.0 *m/s* and angle α = 0, 30, 150, 180, 210 and 330°, relative to the position of a boom with sensor *S*

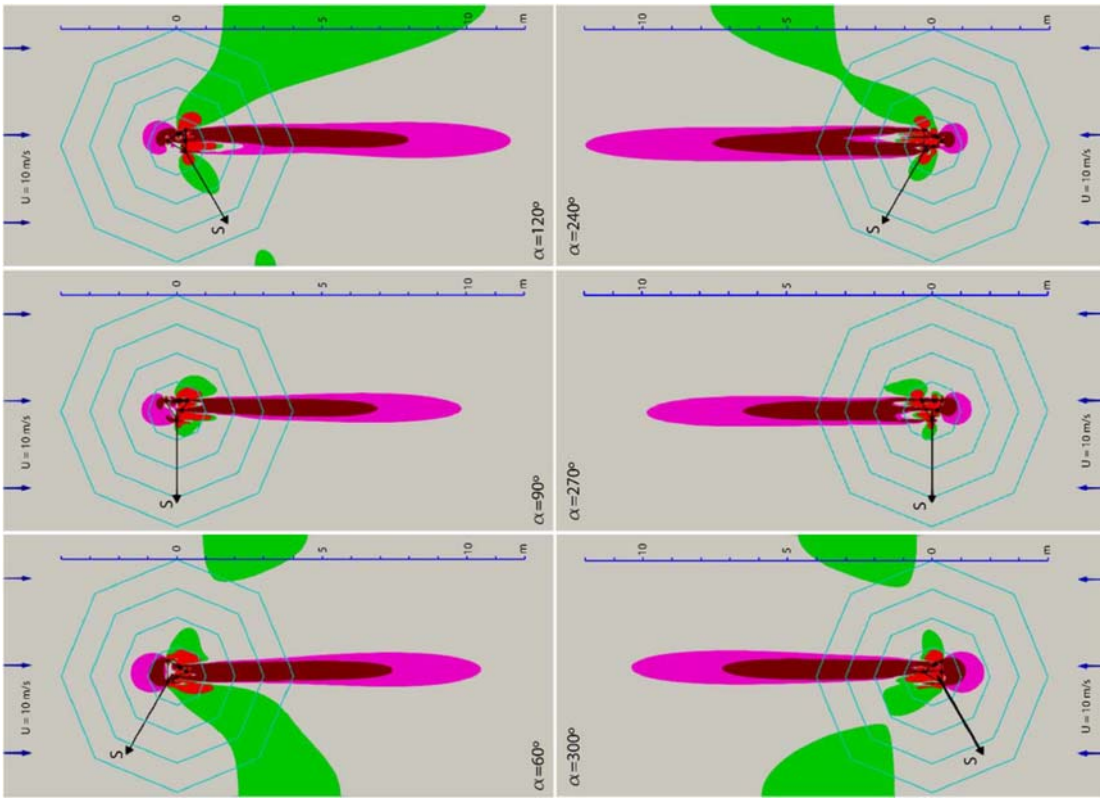

Figure 10 (b). CFD modelling results of the air flow interaction with a triangular lattice mast, side width 0.74 *m*, at the wind speed *U* = 10.0 *m/s* and angle α = 60, 90, 120, 240, 270 and 300°, relative to the position of a boom with sensor *S*

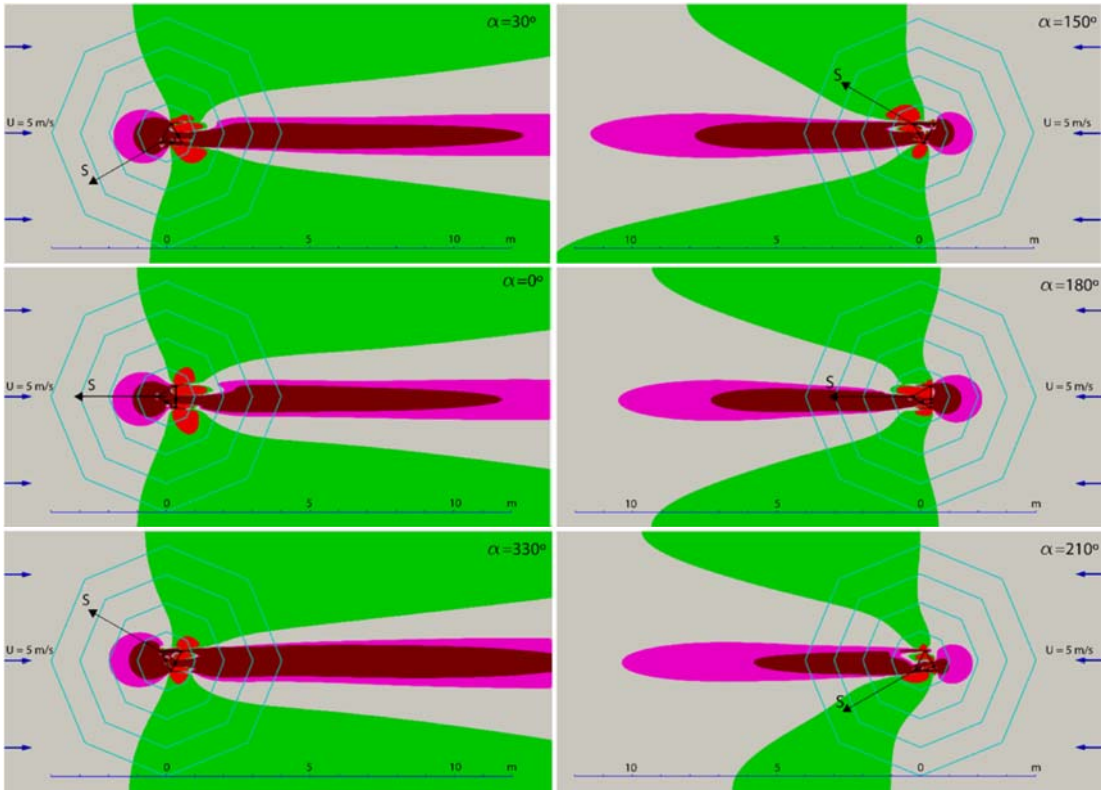

Figure 11 (a). CFD modelling results of the air flow interaction with a triangular lattice mast, side width 0.74 *m*, at the wind speed *U* = 5.0 *m/s* and angle α = 0, 30, 150, 180, 210 and 330°, relative to the position of a boom with sensor *S*

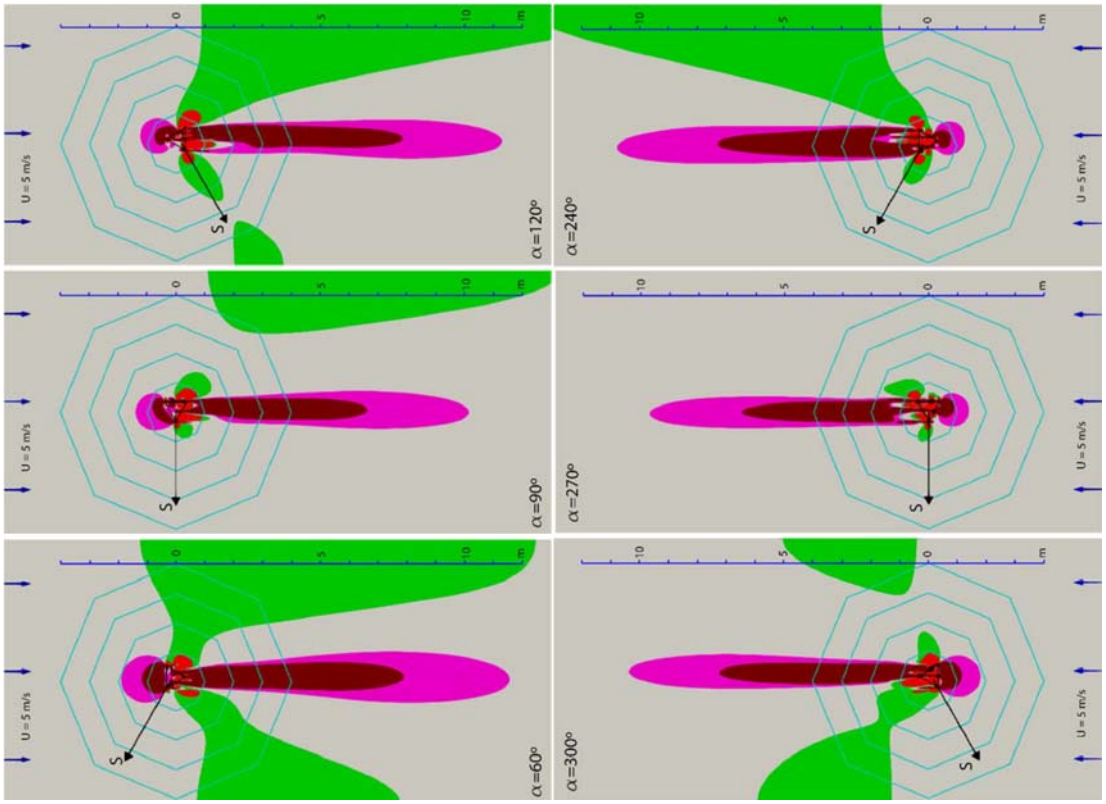

Figure 11 (b). CFD modelling results of the air flow interaction with a triangular lattice mast, side width 0.74 *m*, at the wind speed *U* = 5.0 *m/s* and angle α = 60, 90, 120, 240, 270 and 300°, relative to the position of a boom with sensor *S*

The CFD modelling results are obtained for simulations of air flow interaction with a triangular lattice mast, with side width 0.74 *m*: without taking into account the cable lines at the wind speed *U* = 10.0 *m/s* and angle α = 0°, and taking into account the cable lines at the wind speeds *U* = 5.0 and 10.0 *m/s* at the angles α = 0, 30, 60, 90, 120, 150, 180, 210, 240, 270, 300 and 330° relative to the position of a boom with sensor *S*.

Comparison of the modelling results for wind speeds 5.0 and 10.0 *m/s* shows that with the wind speed increasing the regions where the flow distortion exceeds ± 1.0% becomes smaller.

Presence of cable lines in triangular lattice cellular communication mast slows down the air flow speed greater than 1.5%, which looks like as a narrow train with the length of 10 - 12 sizes of mast side width. In the limits of 350° the region with distortions > ±1.5 % does not exceed the distance of 2 – 3 sizes of mast side width from the centre.

The length of the boom for wind measurements defined by the IEC standard does not guarantee a measurement accuracy of ±1% for measurements in the field of the mast train, while in all other directions the length of the bracket is overestimated.

Acknowledgements

The work is carried out within the project New European Wind Atlas (NEWA), ENER/FP7/618122/NEWA ERA-NET PLUS, supported by the EUROPEAN COMMISSION under the 7th Framework Programme for Research, Technological Development and Demonstration.

References

[1] Bezrukovs V., Bezrukovs Vl., Wind Speed and Energy at Different Heights on the Latvian Coast of the Baltic Sea, *Journal of Energy and Power Sources*. *Vol. 1*, (2014), No. 2, pp. 105-112.

[2] Wind Turbines – Part 12-1: Power Performance Measurements of Electricity Producing Wind Turbines. IEC 61400-12-1, Geneva, Switzerland.

[3] Farrugia R.N., Sant T., Modelling wind speeds for cup anemometers mounted on opposite sides of a lattice tower: A case study, *Journal of Wind Engineering and Industrial Aerodynamics*, *Vol. 115*, (2013), pp. 173–183.

[4] Gioffrè, M., Gusella, V., Materazzi, A. L., Venanzi, I, Removable guyed mast for mobile phone networks: wind load modeling and structural response, *Journal of wind engineering and industrial aerodynamics, Vol. 92*, (2004), pp. 463–475.

[5] Perrin, D., McMahon, N., Crane, M., Ruskin, H. J., Crane, L., Hurley, B., The Effect of Meteorological Tower on its Top-Mounted Anemometer, *Applied Energy, Vol. 84*, (2007), Issue 4, pp. 413-424.

[6] Hansen M., Pedersen B. Influence of the Meteorology Mast on a Cup Anemometer, *Journal of Solar Energy Engineering*, *Vol. 121*, (1999), pp. 128-131.

[7] Stickland, M., Scanlon, T., Fabre, S., Oldroyd, A., & Kindler, D., Measurement and simulation of flow field around a triangular lattice meteorological mast, *Journal of Energy and Power Engineering*, *Vol. 7*, (2013), Issue 10, pp. 1934-1939.

[8] Wibe Mast S1000/1200. www.yumpu.com/en/document/view/18287236/wibe-mast-s1000-1200-scanmast/3

[9] Davidson L. An introduction to turbulence models. Goteborg: Chalmers University of Technology, 2015. 48 p.